

Article type: Full Paper

Deposition of water-stable coatings containing carboxylic acid groups by atmospheric pressure cold plasma jet

Piera Bosso, Fiorenza Fanelli,* Francesco Fracassi

P. Bosso, Prof. F. Fracassi

Department of Chemistry, University of Bari Aldo Moro, via Orabona 4, 70126 Bari, Italy

Dr. F. Fanelli, Prof. F. Fracassi

Institute of Inorganic Methodologies and Plasmas, National Research Council (IMIP-CNR)
c/o Department of Chemistry, University of Bari Aldo Moro, via Orabona 4, 70126 Bari, Italy.

E-mail: fiorenza.fanelli@cnr.it

Thin films containing carboxylic acid groups are deposited from mixtures of helium, acrylic acid and ethylene using an atmospheric pressure cold plasma jet in dielectric barrier discharge (DBD) configuration. The influence of the feed gas composition on the properties of the deposits is investigated. As assessed by X-ray photoelectron spectroscopy (XPS), the oxygen atomic concentration of the coatings as well as the percentage of the XPS C1s component ascribed to carboxylic groups (i.e., COOH and COOR moieties) increase with the acrylic acid concentration in the feed gas. On the other hand, ethylene addition enhances the deposition rate, reduces the carboxylic groups content of the coatings and significantly improves their chemical and morphological stability upon immersion in water for 72 h. The surface concentration of COOH groups before and after immersion in water is determined by chemical derivatization in conjunction with XPS.

Introduction

In the last decade dielectric barrier discharges (DBDs) have attracted growing attention in surface processing of materials, since the atmospheric pressure operation entails simpler equipment design and maintenance with respect to vacuum technology, potentially reducing costs of processes and reactors. One of the main drawbacks of DBDs is the limitation imposed by the narrow gas gaps (usually in the range 0.5-5 mm) on the size and shape of substrates that can be processed directly in the discharge region when, for instance, parallel plate or coaxial cylindrical electrode arrangements are utilized.^[1] To overcome this problem, different types of DBD plasma jets have been developed.^[2,3] Since the plasma is allowed to exit from the region where it is generated, atmospheric pressure plasma jets (APPJs) are ideal for the treatment of substrates with complex shapes and, on the other hand, they can be easily integrated in industrial production lines. Initially, plasma jets were mainly used for surface activation of polymers and metals in order to improve their wettability and adhesion properties,^[4,5] however, recently they have attracted growing interest in thin film deposition.^[6-9] The optimization of the deposition process, i.e. to obtain the desired coating performances with good reproducibility, requires much effort, since many factors can affect the physical and chemical properties of the plasma plume, such as the fluid dynamic conditions, the surrounding environment and the substrate properties.^[9]

Among several plasma-deposited polymers investigated over the last two decades, thin films containing carboxylic acid groups (COOH) have received considerable attention with the aim, for instance, to improve the adhesion of surfaces to polymers or inorganic materials,^[10,11] to enhance cell adhesion and growth,^[12] to increase the adsorption of basic species^[13] and metals.^[14] Deposition processes are mostly performed using acrylic acid (AA) as thin film precursor. Different studies demonstrated that, using both low^[12,15-21] and atmospheric^[22-28] pressure plasmas, it is possible to tune the amount of COOH groups in the coatings by

varying the plasma operational parameters. In particular, at low input power and/or high AA concentration in the feed gas, high percentages of COOH groups can be achieved, comparable to the maximum theoretical value in AA molecule and conventional poly(acrylic acid) (i.e., about 33%),^[12,15,19,23,27, 29] however this is associated with poor water-stability of the coatings, which undergo delamination and preferential removal of carboxylic groups when immersed in water.^[12,15,19] It is worth mentioning that such high COOH concentrations are very often not needed, instead good water-stability of the coatings is required.^[12] As a consequence, one of the main challenges in thin film deposition by AA-containing plasmas is to obtain coatings with good chemical and morphological stability in water. In low pressure plasmas this has been accomplished either by using high input power^[12,17] or through plasma copolymerization (also referred to as codeposition) of AA and another monomer.^[18-21] Several unsaturated hydrocarbons, such as 1,7-octadiene^[18,19], ethylene^[20] and styrene,^[21] were proposed as comonomers: all these molecules have at least one carbon-carbon double bond and act only as cross-linkers and/or chain-extenders, since they do not carry, for instance, new oxygen- or nitrogen-containing functional groups that could be incorporated in the codeposited coating. Few of the studies published to date on the atmospheric pressure plasma deposition from acrylic acid address the issue of coating stability in water. Interestingly, considering the different types of atmospheric discharges utilized, remarkable results were obtained using a pulsed-arc atmospheric pressure plasma jet, that could be defined as a quite-hot thermal plasma source.^[27,28,30,31] The experimental conditions of this plasma jet are carefully optimized to keep the gas temperature low both in the nozzle and downstream of the nozzle (e.g., 1000 K at 10 mm).^[27,28,30,31] This plasma source fed with air/acrylic acid mixtures was utilized by Donegan et al.^[28] to deposit thin films able to enhance protein adhesion. When soaked in an aqueous buffer solution, the coatings showed very low thickness reduction, however after 180 min of water immersion a decrease of the percentage of carboxylic groups (both carboxylic acid and ester groups) from about 25% to about 15% was detected. Arefi and

coworkers used the pulsed-arc plasma jet to obtain thin films with different carboxyl group concentrations and high deposition rates ($1 \mu\text{m min}^{-1}$) from acrylic acid;^[27] however, after 24 h of soaking in water, the coatings showed high delamination associated to weight losses between 50% and 90%. Interestingly, in a recent work, the same authors optimized the plasma copolymerization of AA and methylene-bis-acrylamide to obtain for the first time at atmospheric pressure, water-stable thin films containing both carboxylic and amide functionalities at deposition rates as high as $10 \mu\text{m min}^{-1}$.^[30]

The purpose of this work is the deposition of water-stable coatings containing carboxylic acid groups by an atmospheric pressure cold plasma and, specifically, a cold plasma jet in DBD configuration. First the deposition process was studied using He/AA and He/ethylene feed mixtures, then the codeposition from mixtures containing both AA and ethylene was addressed. It is shown that the addition of ethylene to acrylic acid increases the deposition rate, reduces the concentration of carboxylic groups of the coatings, and significantly improves their water stability. Among others, results from XPS in conjunction with chemical derivatization, and scanning electron microscopy, allow enlightening the chemical and morphological stability of the coatings.

Experimental Section

Thin films were deposited using the atmospheric pressure plasma jet with coaxial cylindrical DBD configuration shown in **Figure 1**. The high voltage (HV) electrode consists of a stainless steel rod (2 mm diameter) placed at the center of a stainless steel cylindrical ground (GND) electrode having inner diameter of 9 mm, length of 50 mm, and externally covered by a Teflon tube. A glass tube (inner diameter of 6 mm, thickness of 1.5 mm, length of 75 mm) is placed between the two electrodes, in direct contact with the ground electrode, and serves as dielectric barrier. The discharge gap corresponds to the 2 mm thick annular space formed

between the HV electrode and the glass tube. The distance between the end of the glass tube and the substrate is set at 5 mm. The plasma jet is located in an airtight Plexiglas box slightly pumped by a diaphragm pump in order to keep the working pressure constant (10^5 Pa) as measured by a MKS baratron.

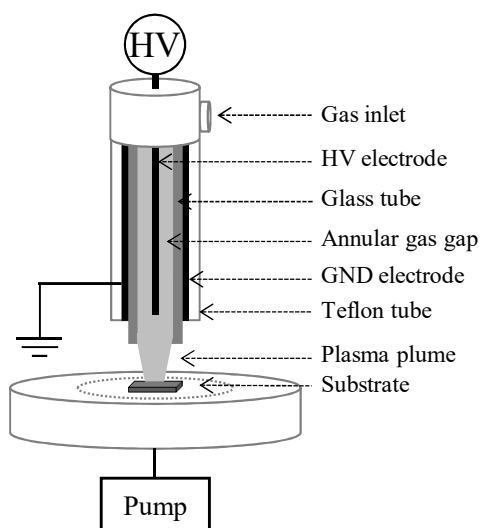


Figure 1. Schematic representation of the atmospheric pressure DBD plasma jet.

The plasma was generated by means of an AC high voltage power supply, composed of a variable frequency generator (TTi TG215), a linear amplifier (Outline PA4006) and a high voltage transformer (Montoux). The excitation frequency (sinusoidal signal) and the applied voltage were set at 20 kHz and 1.4 kV_{rms}, respectively. The discharge was fed with mixtures of He (Air liquide, 99.999%), acrylic acid (2-propenoic acid, Sigma Aldrich, 99%) and ethylene (C₂H₄, Airliquide, 99.95%). The gas flow rates were controlled by MKS electronic mass flow controllers, whereas acrylic acid vapors were introduced into the reactor by a He stream bubbling through a liquid AA reservoir kept at 30°C; the effective amount of AA admitted into the reactor was evaluated by weight variation per unit time of the reservoir and was converted into volumetric flow rate of vapor expressed in sccm, assuming an ideal gas behavior. Deposition processes were carried out for 10 min, keeping constant the He flow rate

at 7 slm, while varying the acrylic acid and ethylene concentrations in the ranges 0 – 25 ppm and 0 – 360 ppm, respectively. Before each experiment the feed mixture was allowed to flow and homogenize for 10 min; this also reduced the air contamination in the Plexiglas box.

The electrical characterization of the discharge was accomplished with a digital oscilloscope (Tektronix TDS2014); the voltage applied to the electrodes was measured by means of a HV probe (Tektronix, P6015) and the discharge current was evaluated by measuring the voltage drop across a 50 Ω resistor connected in series with the ground electrode. The average power dissipated by the discharge was calculated as the integral over one cycle of the product of the applied voltage and the current, divided by the period; a value of 2.0 ± 0.3 W was found in all the investigated conditions.

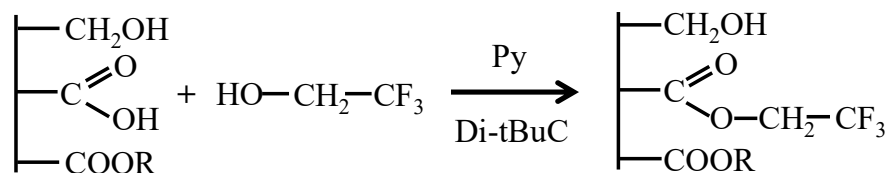
The chemical characterization of the deposited films was carried out by means of X-ray photoelectron spectroscopy (XPS) and attenuated total reflectance Fourier-transform infrared spectroscopy (ATR-FTIR) on coatings deposited onto substrates of c-Si (100) covered with a 700 nm thick layer of SiO₂. XPS analyses were performed by means of a Thermo Scientific Theta Probe spectrometer equipped with a monochromatic Al K α X-ray source (1486.6 eV) operated at a spot size of 300 μ m corresponding to a power of 70 W. Survey (0–1400 eV) and high resolution (C1s, O1s, N1s, Si2p) spectra were recorded at pass energy of 200 and 100 eV, respectively. All spectra were acquired at a take-off angle of 37° with respect to the sample surface, unless otherwise specified. A flood gun was used to balance the surface charging. Charge correction of the spectra was performed by taking the hydrocarbon (C-C, C-H) component of the C1s spectrum as internal reference (binding energy, BE = 285.0 eV).^[32] Atomic percentages were calculated from the high resolution spectra using the Scofield sensitivity factors set in the Thermo Avantage software (Thermo Fisher Corporation) and a nonlinear Shirley background subtraction algorithm. The best-fitting of the high-resolution C1s spectra was performed using the Thermo Avantage software and four components at 285

± 0.2 eV (C-C, C-H), 286.6 ± 0.2 eV (C-OH, C-O-C), 288.1 ± 0.2 eV (O-C-O, C=O), 289.1 ± 0.2 eV (COOH, COOR);^[12] the full-width at half maximum (FWHM) of each C1s component was allowed to vary between 1.3 - 1.6 eV. Reported values are the average of measurements on three different samples (three points for each sample).

The surface concentration of COOH groups was determined by XPS in conjunction with vapor-phase chemical derivatization of COOH groups with trifluoroethanol (TFE). The derivatization reaction is reported in **Scheme 1** and requires the presence of pyridine and N,N'-di-*tert*-butylcarbodiimide as catalyst and drying agent, respectively.^[19,33] The reaction was carried out according to the following procedure:^[19,33] the silicon substrate, on which the coating was deposited, was suspended into a glass round bottom flask, then trifluoroethanol (0.09 mL, Fluka, 99%), pyridine (0.04 mL, Sigma Aldrich, 99%), and N,N'-di-*tert*-butylcarbodiimide (0.03 mL, Sigma Aldrich, 99%) were sequentially added at 15 min intervals into the flask below the silicon substrate. The flask was then sealed with a Teflon cap and the reaction was allowed to proceed at ambient temperature for 14 h. In the case of derivatized samples, the best-fitting of the high-resolution C1s XPS spectra was performed using the following additional component: O-CH₂-CF₃ (287.6 ± 0.2 eV) and CF₃ (293.2 ± 0.2 eV).^[19,32] The COOH concentration, expressed as percentage of the total carbon amount, was calculated according to equation (1):^[21]

$$[\text{COOH}] = \frac{[\text{F}]}{3[\text{C}] - 2[\text{F}]} \times 100 \quad (1)$$

where [C] and [F] are the XPS atomic concentrations of carbon and fluorine of the derivatized sample. Reported values of [COOH] are the average of measurements on three different samples produced in different experiments.



Scheme 1. Derivatization reaction of COOH groups with trifluoroethanol in the presence of pyridine (Py) and N,N'-di-tert-butyl-carbodiimide (Di-tBuC).

Infrared absorption spectra were acquired in the range 375 - 4000 cm^{-1} with a resolution of 4 cm^{-1} in attenuate total reflectance (ATR) mode using a vacuum Bruker Vertex 70v FTIR spectrometer equipped with an ATR module (single reflection diamond crystal). After substrate spectrum subtraction and baseline correction, spectra were normalized to most intense absorption in the 2300-3100 cm^{-1} region.

Static water contact angle (WCA) measurements were carried out by means of a Ramé-Hart manual goniometer (model A-100) using the sessile drop method (double distilled water droplet of 1 μl). Reported values are the average of measurements on three different samples produced in different experiments (four measurements for each sample), with an estimated maximum error of 3°.

Film thickness was evaluated using an Alpha-Step 500 KLA Tencor Surface profilometer and the deposition rate was calculated dividing the average film thickness by the deposition time. The deposit obtained in this process had a circular shape with a diameter of about 8 mm (the glass tube of the DBD jet has a diameter of 6 mm); the thickness of the coatings was measured at the center of the spot within a 4 mm diameter region, unless otherwise specified. Measurements were carried out on three different samples for each experimental condition.

The morphological characterization of the coatings was performed using a Zeiss SupraTM 40 field emission scanning electron microscope (FESEM). SEM images were acquired with the

Everhart–Thornley secondary electron detector at the electron acceleration voltage of 2 kV, working distance of 7.4 mm and tilt angle of 35°. Cross-sectional SEM analyses were carried out after samples fracturing with tweezers using the high resolution in-lens secondary electron detector, at working distance of 5 mm. Samples were sputter-coated with a 10 nm thick layer of Cr prior to SEM observation utilizing a turbo-pumped sputter coater (Quorum Technologies, model Q150T).

In order to compare the results obtained under different experimental conditions, ATR-FTIR, XPS and SEM analyses were carried out in the 4 mm diameter circular region at the center of the deposited spot.

To evaluate the water stability of the coatings, samples were analyzed before and after 72 h of soaking in bidistilled water at room temperature followed by 24 h of drying at ambient conditions.

Results and Discussion

Thin film deposition from mixtures of He/acrylic acid and He/ethylene

Thin films were deposited from He/acrylic acid fed DBDs varying the AA concentration between 10 and 25 ppm. At higher monomer concentrations the discharge could not be safely operated for the formation of localized streamers at the end of the dielectric tube. **Figure 2a** reports the current and voltage signals of a He/acrylic acid fed DBD at [AA] of 19 ppm; the current signal is composed of one main peak and one small secondary peak per half cycle, as for instance in pseudoglow discharges;^[34] all positive (and negative) peaks exhibit almost the same shape, amplitude, and position in the cycle;^[1,34] this signal could be indicative of a homogeneous regime of the discharge, however the formation of microdischarges cannot be completely excluded considering that the HV metallic electrode of the DBD jet is in direct contact with the discharge and this can favor discharge filamentation.^[1]

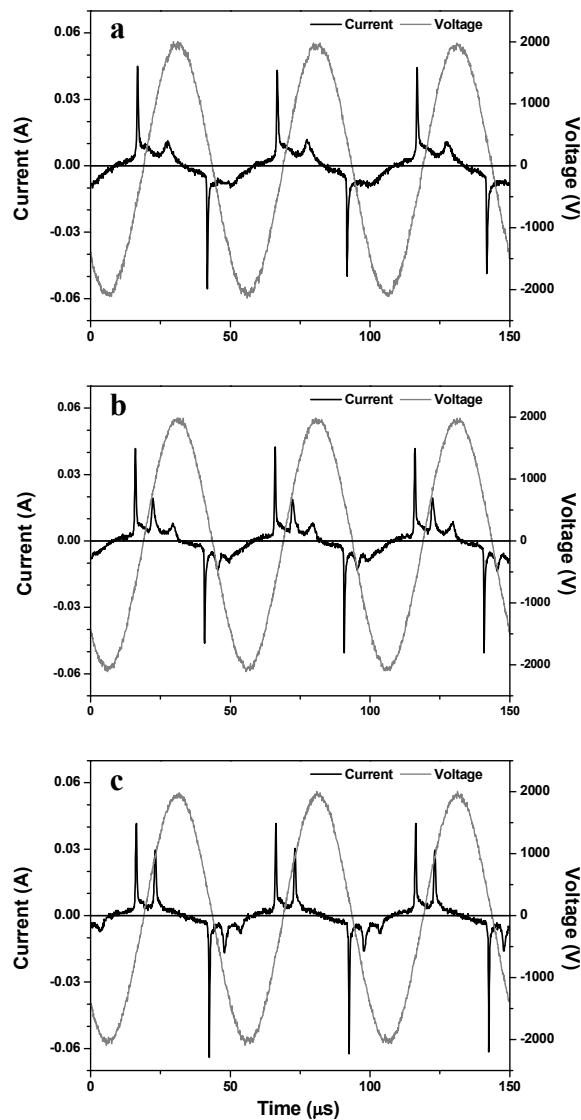


Figure 2. Current and voltage signals of DBD fed by (a) He/ acrylic acid at [AA] = 19 ppm; (b) He/ethylene at [ethylene] = 200 ppm; (c) He/acrylic acid/ethylene at [AA]=19 ppm and [ethylene]= 200 ppm.

With increasing the AA content in the feed, the deposition rate raises from 3.0 ± 0.3 to 20 ± 2 nm min⁻¹, the XPS oxygen atomic concentration of the film increases from $21 \pm 3\%$ to $30 \pm 2\%$, while the area percentage of the XPS C1s component due to carboxylic groups (both COOH and COOR moieties) varies from $4.0 \pm 0.9\%$ to $13.0 \pm 1.0\%$. As it can be seen from the curve-fitted XPS C1s signal in **Figure 3a**, some functional groups which are not contained

in the acrylic acid molecule (e.g., C-O-C, C-OH, C=O, O-C-O) are present in the coatings, reasonably for rearrangement processes following monomer fragmentation.

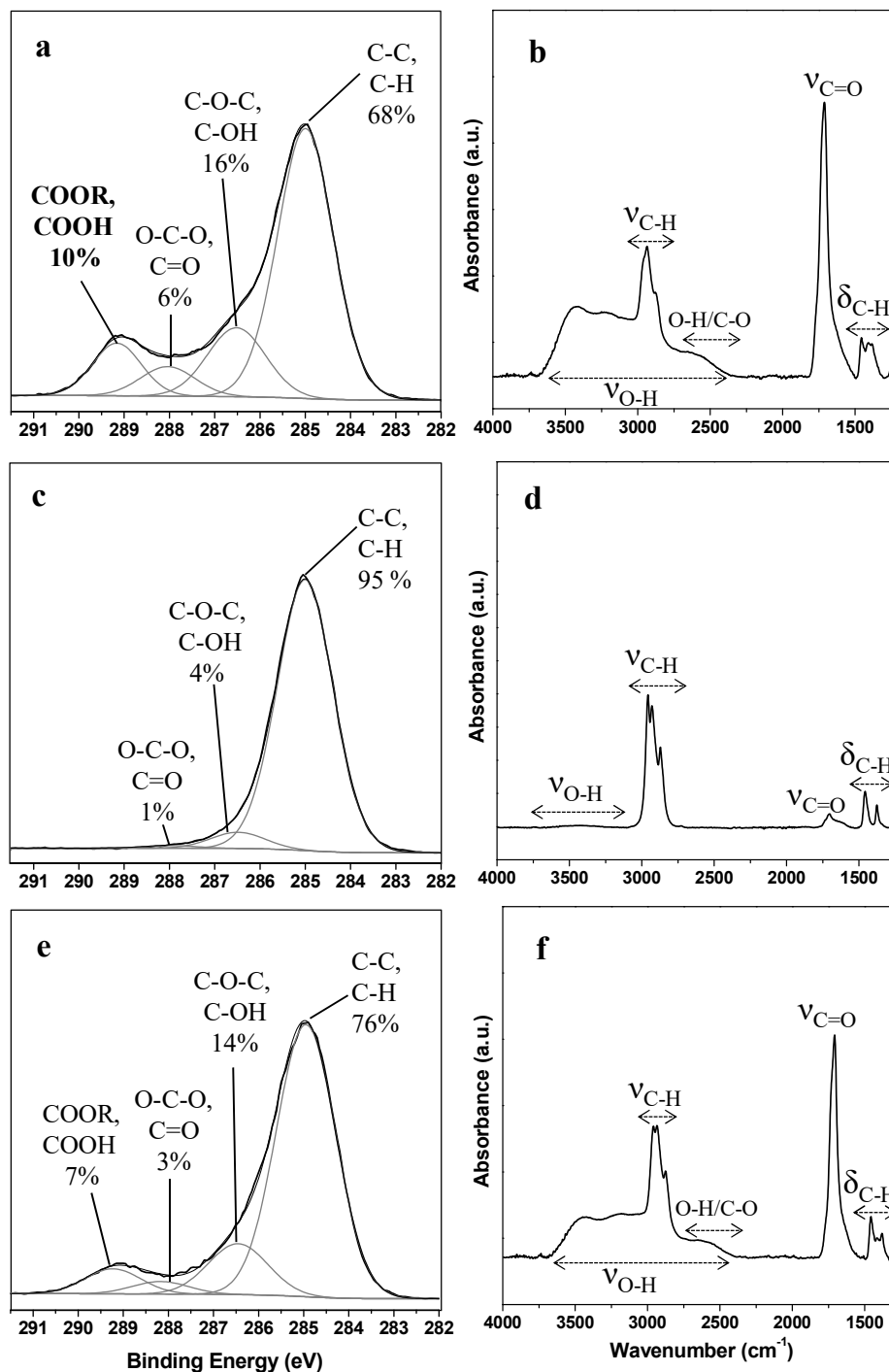


Figure 3. High resolution C1s XPS spectra and ATR-FTIR spectra: (a,b) acrylic acid deposition at [AA] = 19 ppm; (c,d) ethylene deposition at [ethylene] = 200 ppm; (e,f) acrylic acid/ethylene codeposition at [AA]=19 ppm and [ethylene]= 200 ppm.

Figure 3b displays the ATR-FTIR spectrum of the coating obtained at [AA] in the feed of 19 ppm. The main spectral features are^[35,36] the broad OH stretching band between 3700 and 2300 cm^{-1} (due to both carboxylic acid and alcoholic groups), the superimposed CH_x stretching absorptions (3000 – 2800 cm^{-1}), a weak broad band centered at 2640 cm^{-1} ascribable to the combined low frequency vibrations of C-O and O-H in C-OH moieties (associated to both carboxylic acid and alcoholic groups) enhanced by Fermi resonance with the fundamental OH stretching vibration, the C=O stretching peak (1715 cm^{-1}), the CH_x bending absorptions (1500 – 1350 cm^{-1}). The complex profile of the OH stretching band, due to the contributions of different types of OH groups (e.g., OH moieties both in free and H-bonded COOH groups), as well as the absorption band due to the C-O/O-H combined vibrational mode are characteristic of poly(acrylic acid).^[35] XPS and FTIR results indicate that the higher the AA concentration in the feed, the higher is the content of carboxylic groups in the coating; while, as a consequence of the increased content of polar groups, the water contact angle decreases from 46° to 27°. It is worth mentioning that, in case of thin films deposited by He/acrylic acid fed DBDs WCAs measurements provide only indicative values due to the poor water stability of the coatings (as it will be shown herein).

The deposition from He/ethylene mixtures was investigated in the ethylene concentration range 100 - 360 ppm. As shown in Figure 2b, the current signal of a He/ethylene fed DBD at [ethylene] of 200 ppm is composed of one main peak and two weak secondary peak per half cycle, as for instance in pseudoglow discharges.^[34,37] The deposition rate slightly increases from 18 ± 2 to 21 ± 2 nm min^{-1} with the ethylene content, while the XPS oxygen concentration of the coatings decreases from $8.0 \pm 0.7\%$ to $4.0 \pm 0.2\%$ and, consequently, the WCA varies from 90° to 98°. The oxygen content of the coatings can be due to the residual presence of O_2 and H_2O in the deposition chamber and/or to post-deposition uptake upon air exposure.

Figures 3c and 3d report, respectively, the high-resolution XPS C1s signal and the ATR-FTIR absorption spectrum of the deposit obtained at ethylene concentration of 200 ppm. The XPS C1s spectrum is dominated by the aliphatic hydrocarbon component, however weak components due to C-O-C and C-OH functionalities (about 4%) as well as to C=O and O-C-O moieties (about 1%) are also present. The main spectral features in the FTIR spectrum are the band due to C-H stretching in the range 3100-2750 cm⁻¹ and the two signals at 1457 and 1376 cm⁻¹ ascribed to the CH₂ and CH₃ bending, respectively.^[37] Oxygen contamination is also evident, as indicated by the weak absorptions due to OH (band centered at 3400 cm⁻¹) and C=O (1705 cm⁻¹).

Thin film codeposition by acrylic acid and ethylene containing DBD

The codeposition process was firstly carried out at the acrylic acid and ethylene concentrations of 19 and 200 ppm, respectively. The DBD current signal is reported in Figure 2c; the positive cycle consists of two intense peaks, while the negative cycle presents one main peak and two secondary peaks; even if all positive (and negative) peaks exhibit almost the same shape, amplitude, and position in the cycle, a certain filamentation is detected in the discharge gap by naked eye. The best-fitting of the C1s XPS spectrum (Figure 3e) reveals a lower amount of oxygen-containing groups with respect to results obtained with only acrylic acid at the same [AA] in the feed (Figure 3a). Both the XPS oxygen atomic concentration and the peak area percentage of the C1s XPS spectrum ascribed to carboxylic groups are lower for the coating obtained with the codeposition process, i.e. $19.0 \pm 1.0\%$ and $7.0 \pm 0.2\%$, respectively (whereas, with only acrylic acid, $27 \pm 3\%$ and $10 \pm 2\%$, respectively).

The results from the ATR-FTIR investigation are in agreement with XPS analyses. The relative intensities of both OH and C=O bands with respect to the CH_x signal is lower for the coating obtained from helium/acrylic acid/ethylene mixtures (Figure 3f) than from helium/acrylic acid ones (Figure 3b). The presence of the complex broad OH stretching band,

along with the absorption at about 2640 cm^{-1} due to the C-O/O-H combined vibrational mode enhanced by Fermi resonance with OH stretching, suggest that COOH groups are successfully incorporated in the coatings, despite the concentration of acrylic acid in the feed is about one order of magnitude lower than the ethylene one. SEM analyses revealed that coatings obtained from acrylic acid, ethylene and acrylic acid/ethylene mixtures have a smooth and powder-free surface.

The codeposition process was then investigated by varying the concentration of acrylic acid, from 10 ppm to 25 ppm, at a constant [ethylene] of 200 ppm. For AA concentration up to 21 ppm, the deposition rate was in the range $20\text{-}25\text{ nm min}^{-1}$, similar to that obtained with ethylene-fed DBDs without acrylic acid ($20 \pm 3\text{ nm min}^{-1}$); while at [AA] of 25 ppm, it increases to $38 \pm 4\text{ nm min}^{-1}$. As expected, the AA concentration in the feed affects the chemical composition of the coatings. For instance, the XPS atomic concentration of oxygen increases from $13.0 \pm 1.0\%$ to $23 \pm 2\%$ when the AA concentration varied in the range 10-25 ppm. Also the XPS C1s signal is affected by AA addition; in fact, the percentage of the component due to carboxylic groups (both carboxylic acid and ester groups) increases from about 2% to 9% (**Figure 4**) and the peak area percentage ascribed to aliphatic carbon passes from $80 \pm 2\%$ to $74 \pm 2\%$. The same conclusions were reached from ATR-FTIR investigation (spectra not shown) which evidenced an increase of signals due to C=O (1715 cm^{-1}) and OH stretching (3200 cm^{-1}) with respect to the CH_x stretching band. The WCA slightly decreased from 85° to 70° when the acrylic acid concentration was increased from 10 to 25 ppm (**Figure 4b**). It is worth mentioning that the high WCA values obtained for thin film deposited from He/acrylic acid/ethylene fed DBDs suggest a possible reorientation of polar groups likely due to limited cross-linking degree of the coatings. Therefore, WCA measurements were performed as a function of storage time and no appreciable changes in coatings wettability were detected after 1 month of storage. Angle-resolved XPS analyses were also carried out to reveal changes in the chemical composition of the coatings as a function of take-off angle (17,

37 and 57°), i.e., as a function of the sampling depth. For instance, in the case of the as deposited and 1 month aged coatings obtained at [acrylic acid] and [ethylene] in the feed of 19 ppm and 200 ppm, respectively, no variations of the surface chemical composition and of the percentage of the carboxylic groups in the C1s XPS spectra were detected as a function of take-off angle. These evidences allow excluding significant reorientation of polar groups at the surface of the deposited coatings.

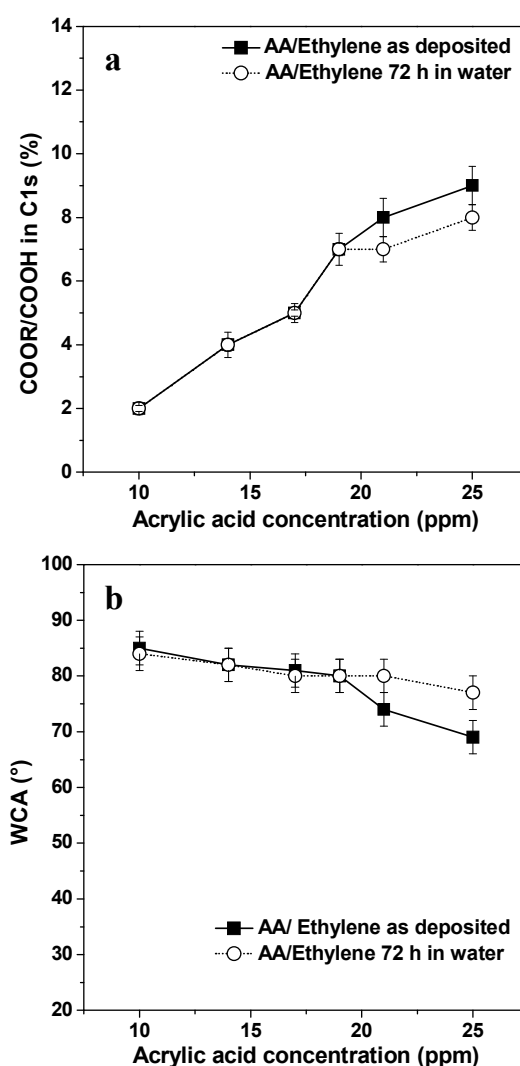


Figure 4. Thin films obtained from acrylic acid/ethylene codeposition as a function of AA concentration, at fixed [ethylene] of 200 ppm: (a) percentage of carboxylic groups in the C1s XPS spectra and (b) WCA for the film before and after 72 h of immersion in water.

The effect of the ethylene concentration was studied in the range 100 – 360 ppm at the constant [AA] of 14 ppm. Deposition rates between $20 \pm 2 \text{ nm min}^{-1}$ and $29 \pm 3 \text{ nm min}^{-1}$ were obtained, with the maximum value at [ethylene] of 300 ppm. These values are higher than that obtained from acrylic acid alone (6 nm min^{-1}). The XPS results at [ethylene] of 100 and 360 ppm are summarized in **Table 1** and indicate that the surface chemical composition of the coatings is not significantly influenced by the ethylene concentration in the feed; however, a slightly increase of the WCA from 80° to 86° was observed at higher ethylene content.

Table 1. XPS atomic concentrations and curve-fitting results of C1s spectra for thin film deposited from He/acrylic acid/ethylene mixtures at [AA] of 14 ppm and [ethylene] concentration of 100 and 360 ppm.

[C ₂ H ₄] (ppm)	C (%)	O (%)	C-H, C-C (%)	C-OH, C-O-C (%)	O-C-O, C=O (%)	COOH, COOR (%)
100	85.2 ± 0.5	14.8 ± 0.5	77.8 ± 1.0	15.0 ± 1.1	3.4 ± 0.3	3.9 ± 0.4
360	84.3 ± 0.5	15.7 ± 0.5	75.6 ± 1.1	16.7 ± 1.2	3.0 ± 0.3	4.7 ± 0.3

Water stability of the coatings

After 72 h of water soaking, the films obtained from He/acrylic acid mixtures showed thickness loss up to 70%, significant reduction of the concentration of carboxylic groups and marked increase of WCA values. In particular with increasing the [AA] in the feed from 10 to 25 ppm, the surface percentage of carboxylic groups assessed by best-fitting of C1s XPS spectra increases from $4.0 \pm 0.9\%$ to 13.0 ± 1.0 for the as deposited coatings, while after immersion in water it increases from $3.0 \pm 0.9\%$ to $8.0 \pm 0.2\%$; on the other hand, the WCA varies in the range $46\text{-}25^\circ$ and $70\text{-}75^\circ$ before and after water immersion, respectively.

On the contrary, the film obtained from ethylene, after 72 h of water soaking showed only a slight increase of the XPS oxygen content, with neither significant change in wettability nor appreciable delamination, as also demonstrated by SEM observations. Also the thin film obtained by the codeposition process generally exhibited good water stability. At the fixed ethylene concentration of 200 ppm, small changes of chemical composition and WCA were detected only for AA concentration higher than 19 ppm (Figure 4). Considering the thin film deposited at AA and ethylene concentrations of 19 and 200 ppm, respectively, **Figure 5a** shows that the percentage of carboxylic groups in the C1s XPS spectra does not change significantly as a function of the position across the deposited spot before and after immersion in water. The thickness profile in Figure 5b is symmetric, shows a maximum at the center of the spot (0 mm position)^[38] and does not change appreciably after water soaking. The thickness loss after 72 h of water soaking was lower than 7% and, in particular, was negligible for AA concentrations up to 19 ppm, as also confirmed by the thickness profile in Figure 5b and the cross-sectional SEM images in Figure 5c.

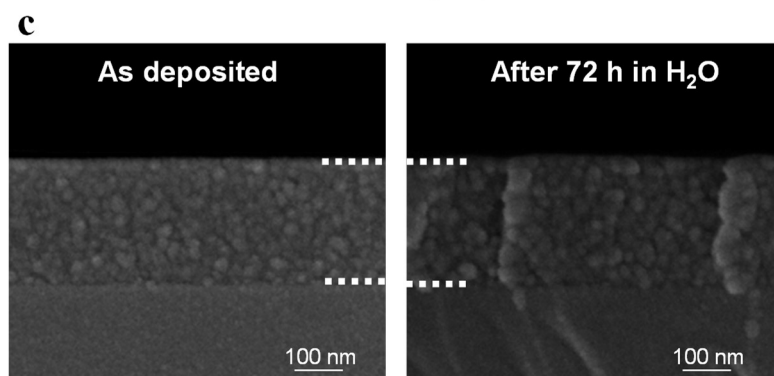
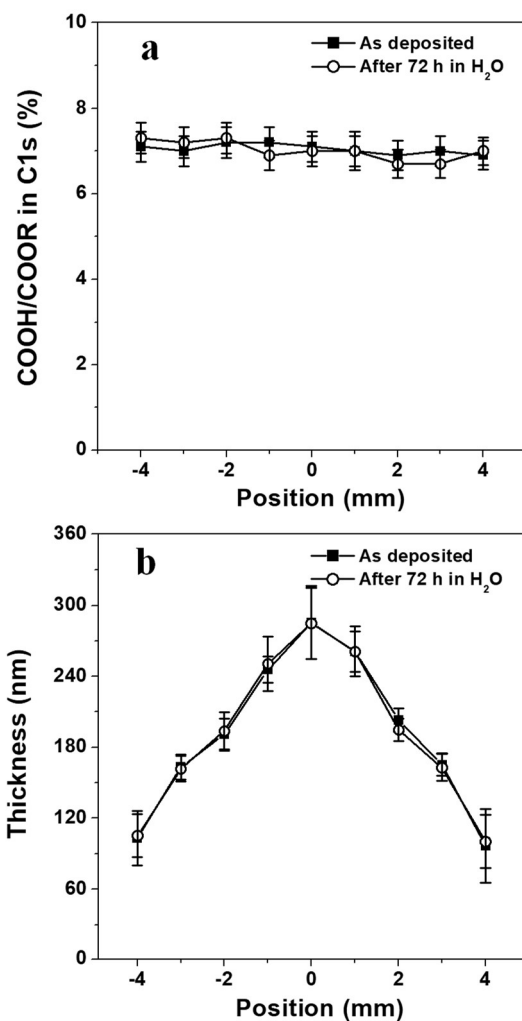


Figure 5. Coating deposited from He/acrylic acid/ethylene fed DBD before and after 72 h water soaking ([AA]= 19 ppm, [C₂H₄] = 200 ppm): (a) profile of the percentage of carboxylic groups in C1s XPS spectra across the deposited spot, (b) thickness profile across the deposited spot, (c) cross-sectional SEM image before and after 72 h water soaking.

Chemical derivatization with trifluoroethanol was carried out in conjunction with XPS analyses to unambiguously estimate the surface concentration of COOH groups of the coatings obtained by DBDs fed with helium/acrylic acid and helium/acrylic acid/ethylene mixtures. As shown in **Figure 6**, after derivatization reaction, the XPS C1s spectrum of the coating obtained from acrylic acid/ethylene codeposition ([AA] and [ethylene] of 19 ppm and 200 ppm, respectively) exhibits two additional components ascribable to O-CH₂-CF₃ (287.6 ± 0.2 eV) and CF₃ (293.2 ± 0.2 eV) functionalities, due to the reaction of trifluoroethanol with COOH groups. The percentage of carboxylic acid groups, as assessed from curve fitting of XPS C1s spectrum after derivatization, is $3.6 \pm 0.5\%$ for the as deposited coating; as reported in **Table 2**, this value remained quite stable after water immersion.

As expected, the COOH percentage of the coating obtained by helium/acrylic acid fed plasma at the same acrylic acid concentration (19 ppm) was higher ($6.8 \pm 1.3\%$) and decreased to $3.2 \pm 0.8\%$ after water soaking. In addition, an intense delamination was also induced by water immersion, leading to a thickness loss of about the 40%.

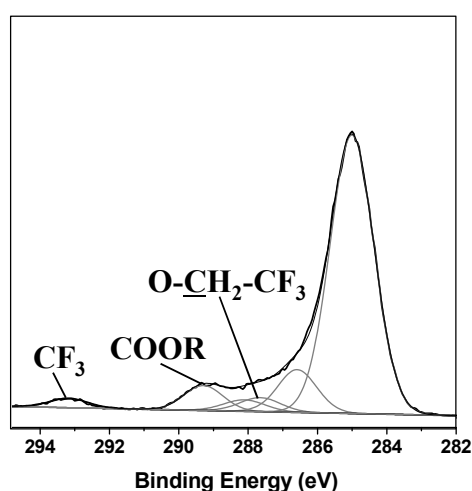


Figure 6. High resolutions C1s XPS spectra after derivatization reaction for AA/ethylene codeposition at [AA]= 19 ppm and [ethylene] = 200 ppm.

Table 2. Water stability of thin films obtained by acrylic deposition and acrylic acid/ethylene codeposition (water immersion for 72 h).

[AA] [ppm]	[Ethylene] [ppm]	Before water immersion		After water immersion		
		COOR+COOH ^{a)}	COOH ^{b)}	COOR+COOH ^{a)}	COOH ^{b)}	Thickness loss
		[%]	[%]	[%]	[%]	
19	200	7.0 ± 0.1	3.6 ± 0.5	6.9 ± 0.5	3.7 ± 0.6	1.0 ± 0.2
19	0	10 ± 2	6.8 ± 1.3	7.6 ± 0.5	3.2 ± 0.8	40.0 ± 1.0
14	0	6.5 ± 0.3	4.6 ± 0.7	3.8 ± 0.4	3.2 ± 0.7	7.0 ± 1.0
25	200	9.0 ± 0.6	6.6 ± 0.6	8.0 ± 0.4	6.1 ± 0.6	7.0 ± 1.0
14	100	3.9 ± 0.4	2.9 ± 0.3	3.8 ± 0.3	3.0 ± 0.2	3.0 ± 0.3
14	360	4.7 ± 0.3	3.2 ± 0.5	4.7 ± 0.3	3.0 ± 0.7	2.0 ± 0.3

^{a)} The percentage of carboxylic groups (COOH+COOR) is assessed by curve-fitting of the C1s XPS spectrum before derivatization reaction; ^{b)}the percentage of COOH groups is determined by XPS analyses after derivatization reaction.

A comparison was also performed between the coatings deposited from acrylic acid (14 ppm), and from a mixture of acrylic acid/ethylene (19 ppm/200 ppm). These coatings are characterized by a similar percentage of carboxylic groups (both COOH and COOR groups) before derivatization, i.e. about 7%. The results reported in Table 2 and **Figures 7a** and **7b** show that for the coating obtained without ethylene, the concentration of carboxylic acid groups and the surface morphology are significantly affected by water immersion; in particular the XPS concentration of COOH decreases from 4.6 ± 0.7% to 3.2 ± 0.7 and SEM observations evidence change in the film morphology. On the contrary, the thin film obtained from AA/ethylene codeposition showed good stability: no reduction of COOH percentage,

negligible thickness loss, and no morphological modifications were observed after water immersion (Figures 7c and 7d).

It is worth highlighting that the thin film deposited by He/acrylic acid/ethylene mixtures at the maximum [AA] of 25 ppm undergoes a very slight decrease of the concentration of COOH groups from 6.6 ± 0.6 to 6.1 ± 0.6 upon immersion in water. (Table 2). Interestingly, coatings obtained at the minimum and maximum [ethylene] of 100 and 360 ppm, respectively (at fixed [AA] of 14 ppm), show a similar [COOH] before and after water soaking (about 3%).

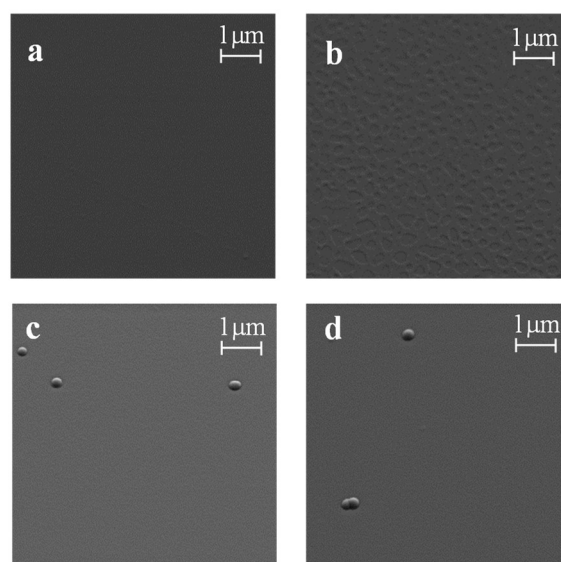


Figure 7. SEM images of thin films obtained from acrylic acid and acrylic acid/ethylene plasma polymerization characterized by similar area percentage of carboxylic groups component (COOR and COOH) in XPS C1s signal before immersion in water (about 7%, Table 2). Acrylic acid deposition: thin film before (a) and after 72 h of soaking in water (b); acrylic acid/ethylene deposition: thin film before (c) and after 72 h of soaking in water (d).

Conclusion

Water-stable coatings were deposited from mixtures containing acrylic acid and ethylene utilizing an atmospheric pressure DBD plasma jet. The incorporation of carboxylic acid

groups in the deposit was demonstrated by FT-IR and XPS, also after derivatization reaction with trifluoroethanol. The acrylic acid concentration in the feed mainly affects the chemical composition of the coating, i.e., the oxygen content and the percentage of carboxylic groups. Ethylene addition mainly increases the deposition rate (up to 29 nm min⁻¹) and reduces the content of carboxylic groups in the coatings. While thin films obtained by plasma fed without ethylene are unstable in water (i.e., loss of carboxylic functionalities, delamination and morphology variation are detected), the coatings deposited from acrylic acid/ethylene mixtures, are very stable and do not show any modification even after 72 h of water immersion, when deposited at AA feed concentration up to 19 ppm.

Acknowledgements: The research was supported by the Italian Ministry for Education, University and Research (MIUR) under grants PONA3_00369, and Regione Puglia under grant no. 51 “LIPP” within the Framework Programme Agreement APQ “Ricerca Scientifica”, II atto integrativo - Reti di Laboratori Pubblici di Ricerca.

Received:; Revised:; Published online:

Key words (max 5): acrylic acid, carboxylic functionalities, deposition, dielectric barrier discharges (DBD), plasma jet

[1] F. Massines, C. Sarra-Bournet, F. Fanelli, N. Naudé, N. Gherardi, *Plasma Process. Polym.* **2012**, *9*, 1041.

[2] M. Laroussi, T. Akan, *Plasma Process. Polym.* **2007**, *4*, 777.

[3] T. Belmonte, G. Henrion, T. Gries, *J. Therm. Spray Technol.* **2011**, *20(4)*, 744.

[4] M.D. Green, F.J. Guild, R.D. Adams, *Int. J. Adhes. Adhes.* **2002**, *22*, 81.

- [5] M. Noeske, J. Degenhardt, S. Strudthoff, U. Lommatzsch, *Int. J. Adhes. Adhes.* **2004**, *24*, 171.
- [6] J. Schäfer, R. Foest, A. Quade, A. Ohl, J. Meichsner, K.D. Weltmann, *Eur. Phys. J. D* **2009**, *54*, 211.
- [7] A. Vogelsang, A. Ohl, R. Foest, K. Schröder, K.-D. Weltmann, *Plasma Process. Polym.* **2011**, *8*, 77.
- [8] Wei-Chun Ma, Ching-Yuan Tsai, Chun Huang, *Surf. Coat. Technol.* **2014**, *259*, 290.
- [9] S. Bornholdt, M. Wolter, and H. Kersten, *Eur. Phys. J. D* **2010**, *60*, 653.
- [10] V. Sciarratta, U. Vohrer, D. Hegemann, M. Muller, C. Oehr, *Surf. Coat. Technol.* **2003**, *174-175*, 805.
- [11] J. Friedrich, R. Mix, R.-D. Schulze, A. Rau, *J. Adhes. Sci. Technol.* **2010**, *24*, 1329.
- [12] L. Detomaso, R. Gristina, G.S. Senesi, R. d'Agostino, P. Favia, *Biomaterials* **2005**, *26*, 3831.
- [13] N. De Vietro, R. d'Agostino, F. Fracassi *Carbon* **2011**, *49*, 249.
- [14] H. Cheng, J. Yu, K. Zeng, G. Hou, *Plasma Process. Polym.* **2013**, *10*, 931.
- [15] R. Jafari, M. Tatoulian, W. Morscheidt, F. Arefi-Khonsari, *React. Funct. Polym.* **2006**, *66*, 1757.
- [16] D. Hegemann, E. Korner, S. Guimond, *Plasma Process. Polym.* **2009**, *6*, 246–254.
- [17] S. Zanini, R. Ziano, C. Riccardi, *Plasma Chem. Plasma Process.* **2009**, *29*, 535.
- [18] R. M. France, R. D. Short, R. A. Dawson, S. MacNeil, *J. Mater. Chem.* **1998**, *8*, 37. [19] M. R. Alexander, T.M. Duc, *Polymer* **1999**, *40*, 5479.
- [20] B.R. Pistillo, *Surf. Coat. Technol.* **2011**, *205*, S534.
- [21] A. Fahmy, R. Mix, A. Schönhals, J. Friedrich, *Plasma Process. Polym.* **2012**, *9*, 273.
- [22] L. J. Ward, W. C. E. Schofield, and J. P. S. Badyal, *Chem. Mater.* **2003**, *15*, 1466.
- [23] A.J. Beck, R.D. Short, A. Matthews, *Surf. Coat. Technol.* **2008**, *203*, 822.

- [24] R. Morent, N. De Geyter, S. Van Vlierberghe, E. Vanderleyden, P. Dubruel, C. Leys, E. Schacht, *Plasma Chem. Plasma Process.* **2009**, *29*, 103.
- [25] M. Okubo, *J. Photopolym. Sci. Technol.* **2008**, *21*, 219.
- [26] G. Chen, M. Zhou, Z. Zhang, G. Lv, S. Massey, W. Smith, M. Tatoulian, *Plasma Process. Polym.* **2011**, *8*, 701.
- [27] O. Carton, D. B. Salem, S. Bhatt, J. Pulpytel, F. Arefi-Khonsari, *Plasma Process. Polym.* **2012**, *9*, 984.
- [28] M. Donegan, D.P. Dowling, *Surf. Coat. Technol.* **2013**, *234*, 53.
- [29] R. Morent, N. De Geyter, M. Trentesaux, L. Gengembre, P. Dubruel, C. Leys, E. Payen, *Appl. Surf. Sci.* **2010**, *257*, 372.
- [30] D. B. Salem, O. Carton, H. Fakhouri, J. Pulpytel, F. Arefi-Khonsari, *Plasma Process. Polym.* **2014**, *11*, 269.
- [31] D. P. Dowling, F. T. O'Neill, S. J. Langlais, V. J. Law, *Plasma Process. Polym.* **2011**, *8*, 718.
- [32] G. Beamson, D. Briggs, *High Resolution XPS of Organic Polymers*, J. Wiley & Sons, Chichester **1992**.
- [33] A. Chilkoti, B. D. Ratner, D. Briggst, *Chem. Mater.*, **1991**, *3*, 51.
- [34] I. Radu, R. Bartnikas, M. R. Wertheimer, *J. Phys. D: Appl. Phys.* **2005**, *38*, 539.
- [35] J. Dong, Y. Ozaki, K. Nakashima, *Macromolecules*, **1997**, *30*, 1111.
- [36] N. A. Atamas, A. M. Yaremko, L. A. Bulavin, V. E. Pogorelov, S. Berski, Z. Latajka, H. Ratajczak, A. Abkowicz-Bienko, *J. Mol. Struct.* **2002**, *605*, 187.
- [37] F. Fanelli, F. Fracassi, R. d'Agostino, *Plasma Process. Polym.* **2005**, *2*, 688.
- [38] C. Merten, C. Regula, A. Hartwig, J. Ihde, R. Wilken, *Plasma Process. Polym.* **2013**, *10*, 60.

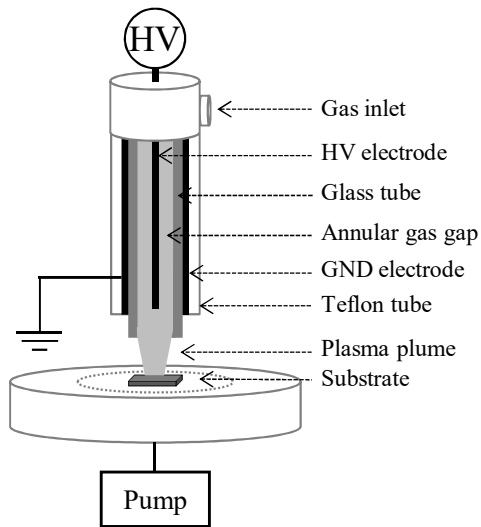


Figure 1. Schematic representation of the atmospheric pressure DBD plasma jet.

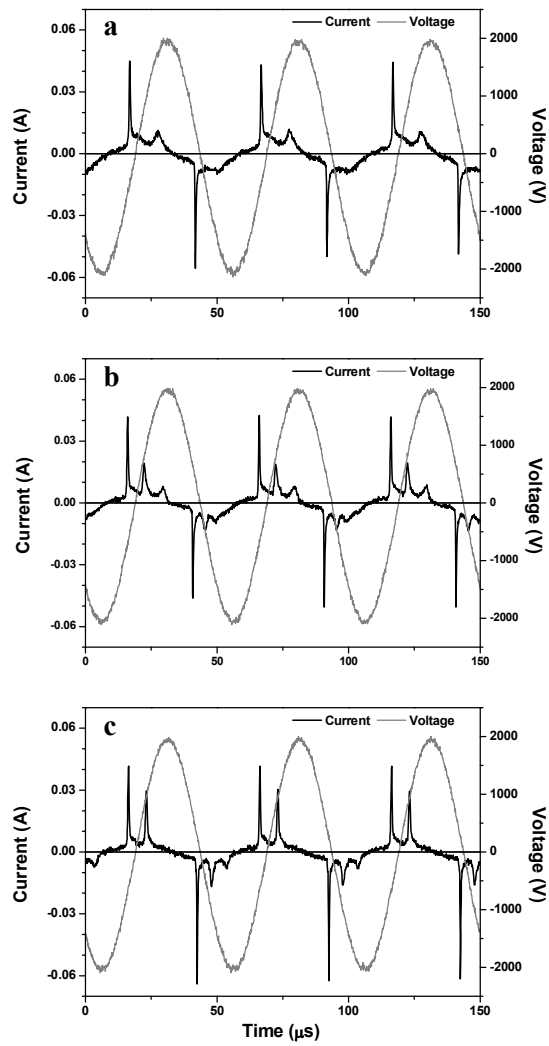


Figure 2. Current and voltage signals of DBD fed by (a) He/ acrylic acid at [AA] = 19 ppm; (b) He/ethylene at [ethylene] = 200 ppm; (c) He/acrylic acid/ethylene at [AA]=19 ppm and [ethylene]= 200 ppm.

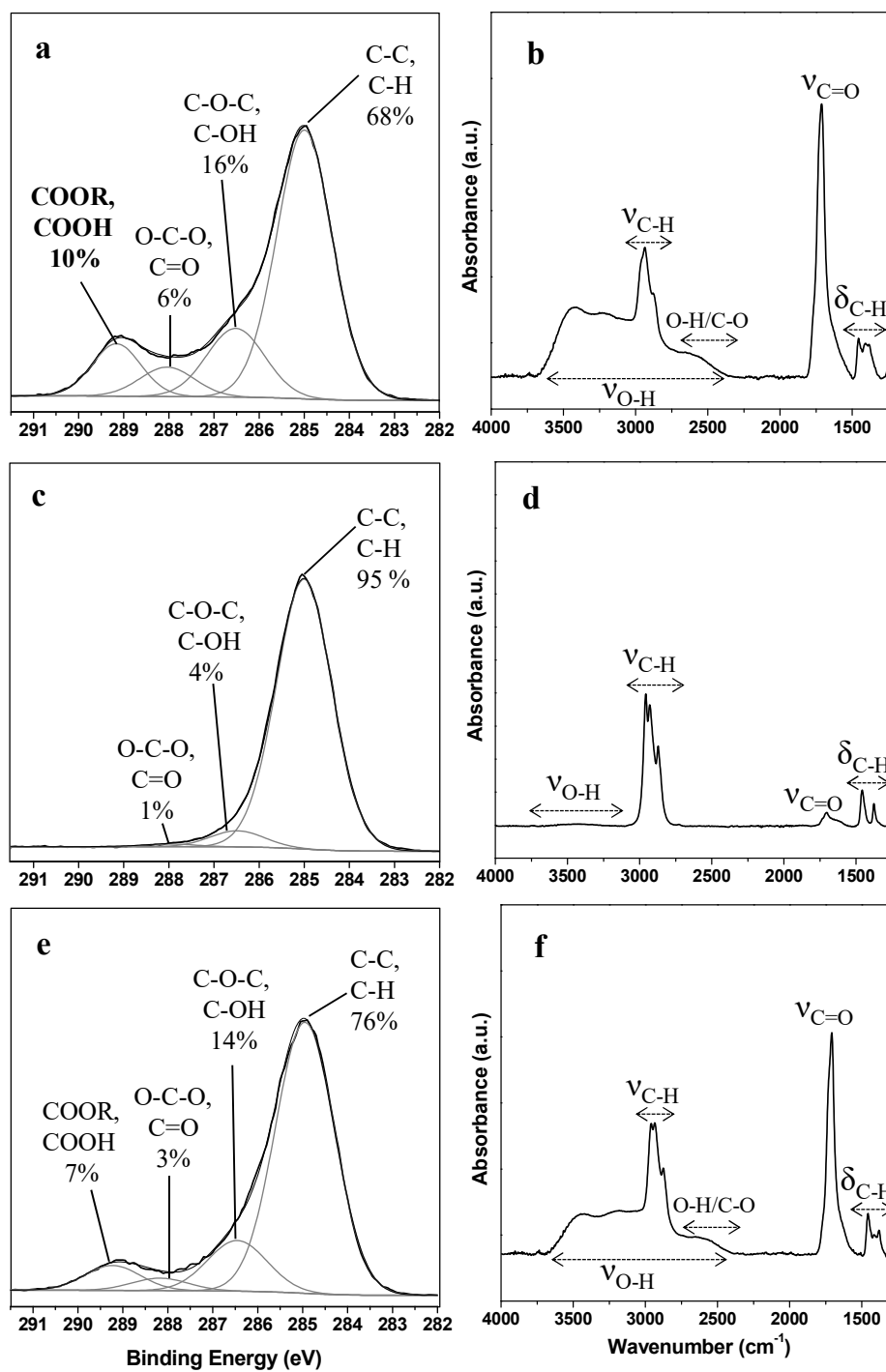


Figure 3. High resolution C1s XPS spectra and ATR-FTIR spectra: (a,b) acrylic acid deposition at [AA] = 19 ppm; (c,d) ethylene deposition at [ethylene] = 200 ppm; (e,f) acrylic acid/ethylene codeposition at [AA]=19 ppm and [ethylene]= 200 ppm.

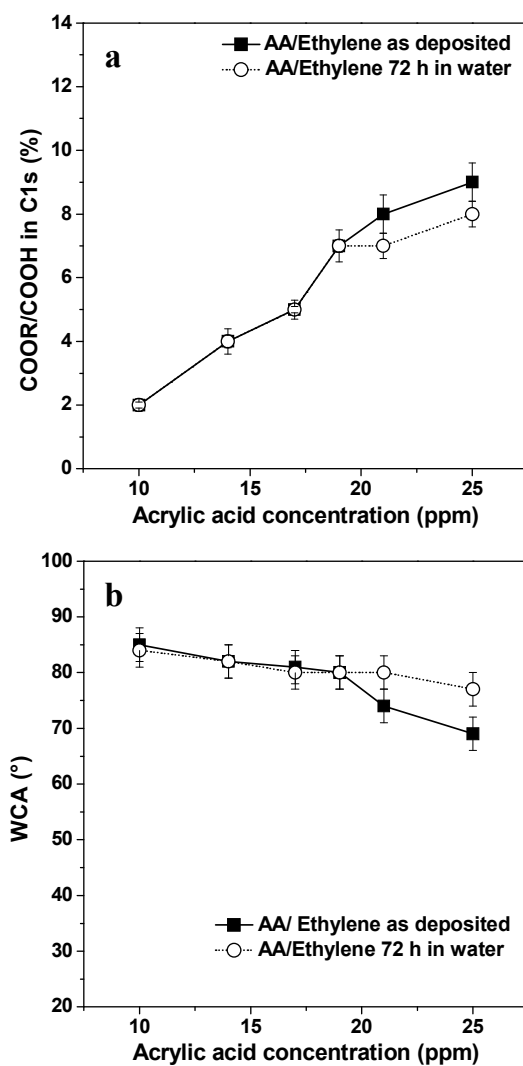


Figure 4. Thin films obtained from acrylic acid/ethylene codeposition as a function of AA concentration, at fixed [ethylene] of 200 ppm: (a) percentage of carboxylic groups in the C1s XPS spectra and (b) WCA for the film before and after 72 h of immersion in water.

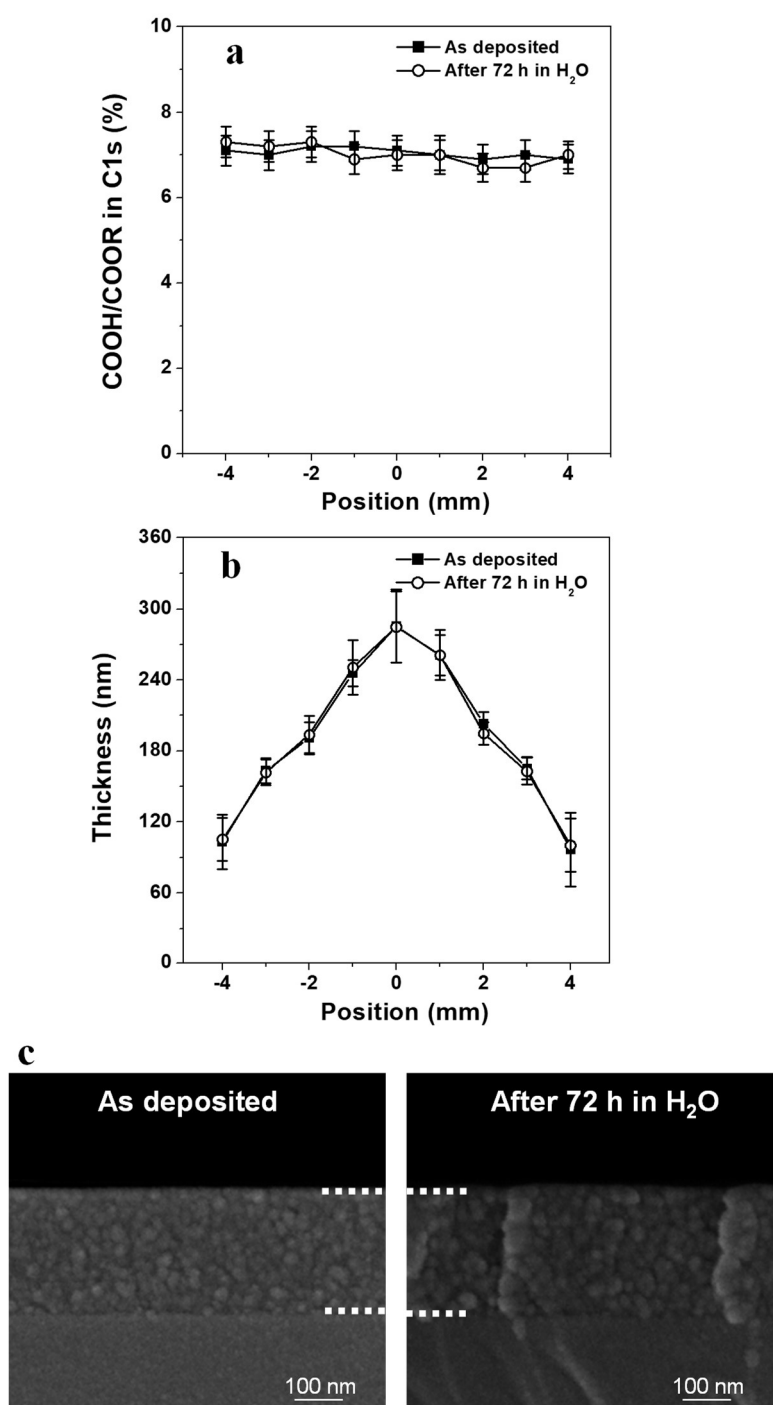


Figure 5. Coating deposited from He/acrylic acid/ethylene fed DBD before and after 72 h water soaking ([AA]= 19 ppm, [C₂H₄] = 200 ppm): (a) profile of the percentage of carboxylic groups in C1s XPS spectra across the deposited spot, (b) thickness profile across the deposited spot, (c) cross-sectional SEM image before and after 72 h water soaking.

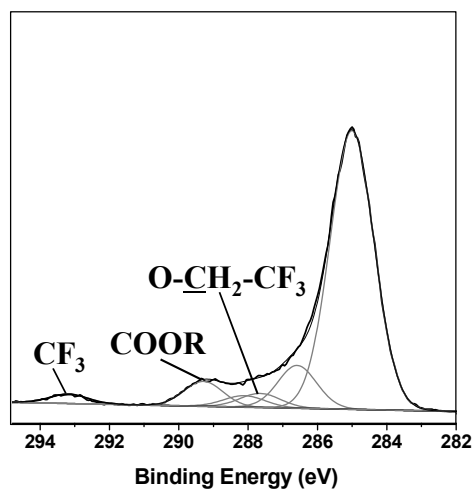


Figure 6. High resolutions C1s XPS spectra after derivatization reaction for AA/Ethylene codeposition at [AA]= 19 ppm and [ethylene] = 200 ppm.

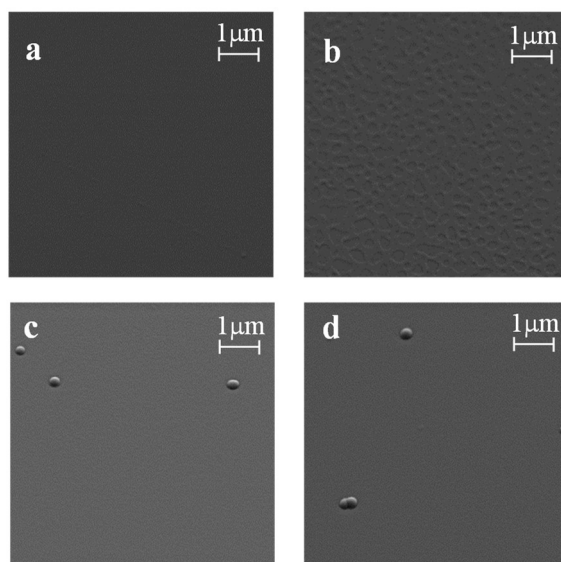


Figure 7. SEM images of thin films obtained from acrylic acid and acrylic acid/ethylene plasma polymerization characterized by similar area percentage of carboxylic groups component (COOR and COOH) in XPS C1s signal before immersion in water (about 7%, Table 2). Acrylic acid deposition: thin film before (a) and after 72 h of soaking in water (b); acrylic acid/ethylene deposition: thin film before (c) and after 72 h of soaking in water (d).

In this work an atmospheric pressure DBD plasma jet fed with helium, acrylic acid and ethylene is used to deposit thin films containing carboxylic acid groups. The addition of ethylene to the feed mixture increases the deposition rate, reduces the carboxylic groups content of the coatings and significantly improves their chemical and morphological stability upon immersion in water.

P. Bosso, F. Fanelli,* F. Fracassi

Deposition of water-stable coatings containing carboxylic acid groups by atmospheric pressure cold plasma jet

